

1 Dear Referees,

2 Thanks for giving us an opportunity to revise our manuscript (acp-2019-1045). We appreciate your positive and con-  
3 structive comments. We have studied these comments carefully and make revisions on the manuscript. These com-  
4 ments and the corresponding replies are listed below.

5 The referee's comments are highlighted by gray. The symbol ">>" quotes the original texts in the manuscript. Followed  
6 by the comments are our responses (normal texts) and current texts in the manuscript (leaded by **line number**). Some  
7 important revisions are colored by red. The revised manuscript with track changes are attached at the end of this file.

8 With regards,

9 Shuqi Yan, Bin Zhu\*, and all co-authors.

10

11

## 12 **Replies to Referee#1**

13 **1.** Line 37-38: As indicated in IPCC AR5, “aerosol-cloud-radiation interactions” is suggested to be rephrased as “aero-  
14 sol-radiation interaction” and “aerosol-cloud interaction” separately.

15 >>Line 37-38: ...which are called as aerosol-cloud-radiation interactions...

16 Thank you for this valuable suggestion. We have corrected it.

### 17 **Line 38-39 (Introduction)**

18 ...which are called as aerosol-radiation and aerosol-cloud interactions...

### 19 **Line 458 (Table 1)**

20 Aerosol-cloud-radiation interactions --> Aerosol-cloud and aerosol-radiation interactions

21

22 **2.** Line 41: “Many”->“Previous”

23 >>Line 41: Many studies have analysed...

24 Thank you for this valuable suggestion. We have changed all the "many studies" to "previous studies" (Line 35, 42,  
25 219).

26

27 **3.** Line 45: "lower supersaturation" ??

28 >>Line 45: As a result, urban areas commonly experience higher temperatures and lower vapour contents. These condi-  
29 tions induce a **lower supersaturation** that is unfavourable for fog formation.

30 Thank you for this valuable suggestion. We have corrected this sentence.

31 **Line 46 (Introduction)**

32 ...These conditions induce a **lower relative humidity** supersaturation that is unfavourable for fog formation.

33

34 **4.** Lines 64-65: Some important references are missing regarding the observational evidences of aerosol boomerang  
35 effect in China, e.g., Wang et al., AE 2015, doi: 10.1016/j.atmosenv.2015.04.063; Guo et al., GRL 2017, doi:  
36 10.1002/2017GL073533; Liu et al., Sci. Rep. 2019, doi:10.1038/s41598-019-44284-2.

37 >>Lines 64-65: However, if aerosol concentration exceeds a certain threshold, this promoting effect disappears (Quan  
38 et al., 2011) or even turns into a suppressing effect due to the strong vapour competition (**Koren et al., 2008;**  
39 **Rangognio, 2009**).

40 Thank you for this valuable suggestion. We have added these references to the end of this sentence.

41 **Line 68 (Introduction)**

42 .....or even turns into a suppressing effect due to the strong vapour competition (**Guo et al., 2017; Koren et al.,**  
43 **2008; Liu et al., 2019; Rangognio, 2009; Wang et al., 2015**).

44

45 **5.** Lines 69-71: I notice that the work by Yan et al. JGR (2019) mentioned here is also from the same research group.  
46 Also, it occurs to me that the motivation seems a little confused: Since previous work has "quantitatively" proved...

47 why the authors attempt again to “quantitatively” confirm by model simulation of a fog event. Two “quantitatively ” is  
48 redundant. Therefore, this sentence is suggested to be rephrased as follows: e.g. Our recent observational work (Yan et  
49 al., 2019) indicated a decreasing trend in fog days, and ...”

50 >>Lines 69-71: Yan et al. (2019) analysed decadal trends of fog days and quantitatively proved that the inhibiting ef-  
51 fects of urbanization outweigh the promoting effects of aerosols on fog during the mature urbanization stage. Their  
52 study inspires us to quantitatively confirm the roles of urbanization and aerosols.....

53 Thank you for this valuable suggestion. The redundant “quantitatively” is deleted. We have corrected this sentence.

54 **Line 72-76 (Introduction)**

55 Our recent observational work (Yan et al., 2019) indicated a decreasing trend in fog days, and the inhibiting ef-  
56 fects of urbanization outweigh the promoting effects of aerosols on fog during the mature urbanization stage. This  
57 study aims to quantitatively confirm the roles of urbanization and aerosols.....

58

59 **6. Line 75: “facilitates”-> “is expected to facilitate”**

60 >>Line 75: This work facilitates the understanding of.....

61 Thank you for this valuable suggestion. We have corrected these sentences.

62 **Line 79 (Introduction)**

63 This work is expected to facilitate the understanding of...

64 **Line 305 (Conclusions)**

65 This study is expected to facilitate a better understanding of...

66

67 **7. Line 85: Something is suggested to be mentioned concerning Section 4 immediately after “Section 3.6 discusses the  
68 rationality and reliability of the results.”**

69 >>Line 85: Section 3.6 discusses the rationality and reliability of the results.

70 Thank you for this valuable suggestion. We have added something after it.

71 **Line 89-90 (Introduction)**

72 Section 3.6 discusses the rationality and reliability of the results. **Section 4 concludes the findings of this study.**

73

74 **8.** Line 90: it is suggested to clarify which city you are referring to? Since the reader cannot easily get any info from  
75 either text or Figure 1b.

76 >>Line 90: SX is ... approximately 30 km away from the nearest large city (Fig. 1b).

77 Thank you for this valuable suggestion. We have clarified this city, Huainan. It has been marked in Figure 1b.

78 **Line 95 (Section 2.1)**

79 SX is ... approximately 30 km away from the nearest large city, **Huainan (Fig. 1b).**

80

81 **9.** Line 97: “replace”-> “used to replace”

82 >>Line 97: The data are resampled from 500 m to 30 arc-seconds (approximately 1 km) and **replace** the geological data  
83 of the WRF model.

84 Thank you for this valuable suggestion. We have corrected this sentence.

85 **Line 102 (Section 2.1)**

86 The data are resampled from 500 m to 30 arc-seconds (approximately 1 km) and **used to replace** the geological  
87 data of the WRF model.

88

89 **10.** Lines 160-165: The logic seems a little problematic: since the fog holes are mainly caused by urbanization, as  
90 demonstrated in the references in this paragraph (aerosol effect is not mentioned and is supposed to not be the focus  
91 here), why you mentioned the effect of aerosol pollution. It is generally thought that urbanization effect tends to reduce

92 LWP whereas aerosol tends to accumulate the formation of fog. The combined effect is highly dependent on the com-  
93 peting effect of the two factors. Here it is not accurate to argue that both of them “reducing the LWP or advancing the  
94 dissipation of fog”.

95 >>Line 160-165: ..... We assume that **urbanization and air pollution** could have profound effects on fog by reducing  
96 the LWP or advancing the dissipation of fog.

97 Thank you for this valuable suggestion. We agree that fog holes are mainly caused by urbanization, not by aerosols.  
98 We aimed to express that "the combined effects of urbanization and aerosols lead to fog holes", not "both of them lead  
99 to fog holes". To avoid the problem you mentioned, we have corrected the last sentence.

#### 100 **Line 169-170 (Section 3.1)**

101 We assume that **urbanization** could have profound effects on fog by reducing the LWP or advancing the dissipa-  
102 tion of fog, **and the role of aerosols on fog is weaker than that of urbanization.**

103

104 **11. Section 3.2: What are the criteria for you to determine a fog event from model-simulated LWP, which is required to**  
105 **be clarified here.**

106 Thank you for this valuable suggestion. The criteria for fog is  $LWP > 2 \text{ g/m}^2$  (Jia et al., 2018). We have clarified it in  
107 Section 3.2.

#### 108 **Line 173 (Section 3.2)**

109 Satellite cloud image and modelled LWP ( **$> 2 \text{ g/m}^2$** ) can represent the observed and simulated fog zone (Jia et al.,  
110 2018).

#### 111 **References**

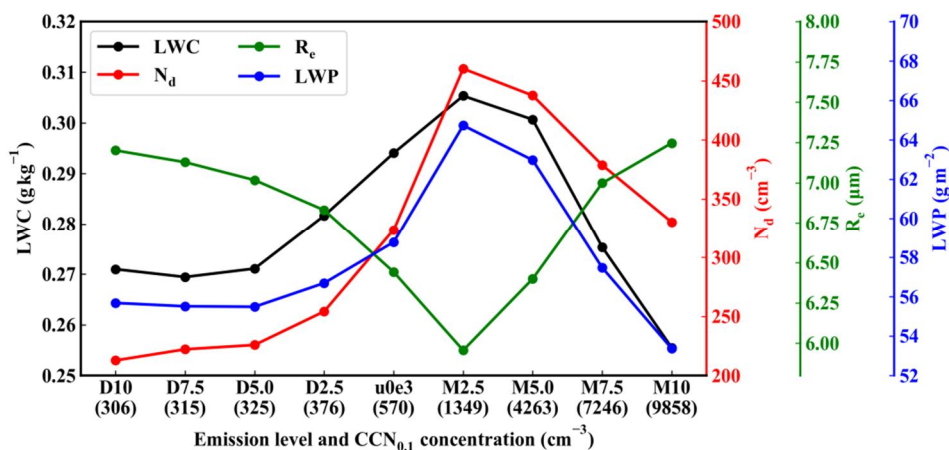
112 Jia, X., Quan, J., Zheng, Z., Liu, X., Liu, Q., He, H., and Liu, Y.: Impacts of anthropogenic aerosols on fog in North China Plain, *J. Ge-*  
113 *ophys. Res.-Atmos.*, 124, 252–265, <https://doi.org/10.1029/2018jd029437>, 2018.

114

115 **12.** Section 3.3: The authors attempted to discuss the complicated non-monotonic effect of aerosol on fog formation by  
 116 differing the emission rate, which is not very common. Why not used the aerosol concentration or CCN or Na that can  
 117 well represent the real atmospheric pollution level for the time period investigated here? I am curious of the actual  
 118 CCN or Na concentration for the experiment of u0e3?

119 Thank you for this valuable suggestion. We agree that CCN can better represent the air pollution level. The  $CCN_{0.1}$   
 120 concentration of each experiment is marked in the new Figure 8, because the supersaturation in fog is commonly less  
 121 than 0.1% (Mazoyer et al., 2016). The  $CCN_{0.1}$  of current pollution level (u0e3) is  $570\text{ cm}^{-3}$ .

122 **Line 510-514 (Figure 8)**



123  
 124 Figure 8. Relationships of the microphysical parameters (LWC,  $N_d$ ,  $R_e$  and LWP) with emission level and  $CCN_{0.1}$  con-  
 125 centrations. These parameters are the time-height averages (time average for the LWP) in fog.

126 **References**

127 Mazoyer, M. , Burnet, F. , Roberts, G. C. , Haefelin, M. , & Elias, T. (2016). Experimental study of the aerosol impact on fog microphys-  
 128 ics. Atmospheric Chemistry and Physics, 1-35.

129  
 130 **13.** Lines 215-216: It will be misleading for the statement “the current pollution level in China is still located in the  
 131 promoting regime rather than the suppressing regime of fog occurrence”. Both ideal simulation (e.g., Rosenfeld et al.  
 132 Science, 2008) or observational studies (Wang et al., AE 2015; Guo et al., GRL 2017) indicated that the tipping point

tends to occur at AOD of 0.3-0.4 or CCN concentration of 1200/cm<sup>3</sup>. Recent observational work by Ilan Koren et al. (Science, 2014) suggested the cloud and precipitation is most sensitive to aerosol over the South Ocean. By comparison, the average AOD from MODIS in East China is on average much larger than 0.6, irrespective of the meteorological conditions.

>>Lines 215-216: The aerosol concentration of the transition point (experiment M2.5) is higher than that of u0e3 (Fig. 8), revealing that **the current pollution level in China is still located in the promoting regime** rather than the suppressing regime of fog occurrence.

Thank you for this valuable suggestion. The CCN<sub>0.4</sub> of u0e3 is 6023 cm<sup>-3</sup>, higher than CCN<sub>0.4</sub>=1200 cm<sup>-3</sup> that revealed by Rosenfeld et al. (Science, 2008). We agree that the AOD value of East China is larger than 0.6. It seems that the current pollution level could suppress fog rather than promotes fog.

The studies you listed mostly aim at convective clouds. Aerosols affect convective clouds through two competing mechanisms: 1) invigorating convection by promoting vapor condensation. 2) suppressing convection by blocking solar radiation and reducing surface heat flux. Under polluted conditions (AOD>0.3 or CCN<sub>0.4</sub>>1200 cm<sup>-3</sup>), the suppressing effect outweighs the invigoration effect, so the turning point occurs (Koren et al. Science, 2008; Rosenfeld et al., Science, 2008). This suppressing effect does not exist in fog because fog commonly formed at night. Therefore, the turning point in fog might occur later than that in convective clouds. In North China Plain where air pollution is thought to be more serious, a case study by WRF-Chem also indicates that fog properties (e.g., LWC, N<sub>d</sub> and LWP) increase monotonically when emission intensity varies from 0.05-fold to 1-fold. It is consistent with our statement "the current pollution level in China is still located in the promoting regime rather than the suppressing regime of fog occurrence".

The above discussions have been included at the end of Section 3.4. Additionally, some statements are given in a more cautious manner.

#### **Line 223-231 (Section 3.4)**

Rosenfeld et al. (2008) revealed that the turning point of boomerang pattern in convective clouds is CCN<sub>0.4</sub> = 1200 cm<sup>-3</sup>. The CCN<sub>0.4</sub> of u0e3 is 6023 cm<sup>-3</sup>, which seems to suppress fog. Aerosols affect convective clouds through two competing mechanisms: 1) invigorating convection by promoting vapour condensation. 2) suppressing convection by blocking solar radiation and reducing surface heat flux. Under polluted conditions (AOD>0.3

160 or  $CCN_{0.4} > 1200 \text{ cm}^{-3}$ ), the suppressing effect outweighs the invigoration effect, so the turning point occurs  
161 (Koren et al., 2008; Rosenfeld et al., 2008). This suppressing effect does not exist in fog because fog commonly  
162 formed at night. Therefore, the turning point in fog might occur later than that in convective clouds. In North Chi-  
163 na Plain where air pollution is thought to be more serious, a case study by WRF-Chem also indicates that fog  
164 properties (e.g., LWC,  $N_d$  and LWP) increase monotonically when emission intensity varies from 0.05-fold to 1-  
165 fold.

166 **Line 220-222 (Section 3.4)**

167 ...~~revealing that~~ possibly indicating that the current pollution level is still located in the promoting regime...

168 **Line 25 (Abstract)**

169 ...the current pollution level in China ~~is-could be~~ still below the critical aerosol concentration that suppresses fog.

171 **14.** Lines 205-206: times is redundant and should be removed.

172 >>Lines 205-206: For example, the name M2.5 means multiplying by 2.5 times; the name D10 means dividing by 10  
173 times.

174 Thank you for this valuable suggestion. We have corrected this sentence.

175 **Line 210 (Section 3.4)**

176 For example, the name M2.5 means multiplying by 2.5; the name D10 means dividing by 10.

178 **15.** Line 448: it is better to indicate the year of 2017 following 03 January in the figure caption.

179 >>Line 448: Figure 2. The performance of the simulated fog zone at 08:00 03 January.

180 Thank you for this valuable suggestion. We have changed two figure captions.

181 **Line 475 (Figure 2)**

182 The performance of the simulated fog zone at 08:00 03 January 2017....



183 **Line 482 (Figure 3)**

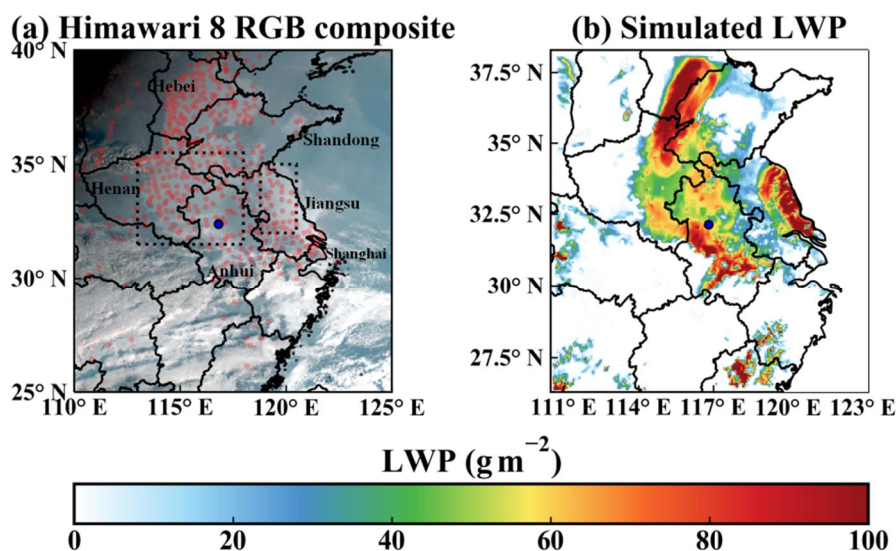
184 Two sub-regions (a and b) with obvious fog holes on the Himawari 8 image at 11:00 03 January 2017....

185

186 **16.** Figure 3: it is suggested to show the major cities in the regions of interest shown in panel a and b, given the con-  
187 venience to better understand the fog hole induced by urban. Besides, two subregions in Figure 3 is better to be marked  
188 in Figure 1 or 2.

189 Thank you for this valuable suggestion. The subregions of interest are marked in the new Figure 2. The cities with fog  
190 holes are marked in the new Figure 3.

191 **Line 473-478 (Figure 2)**

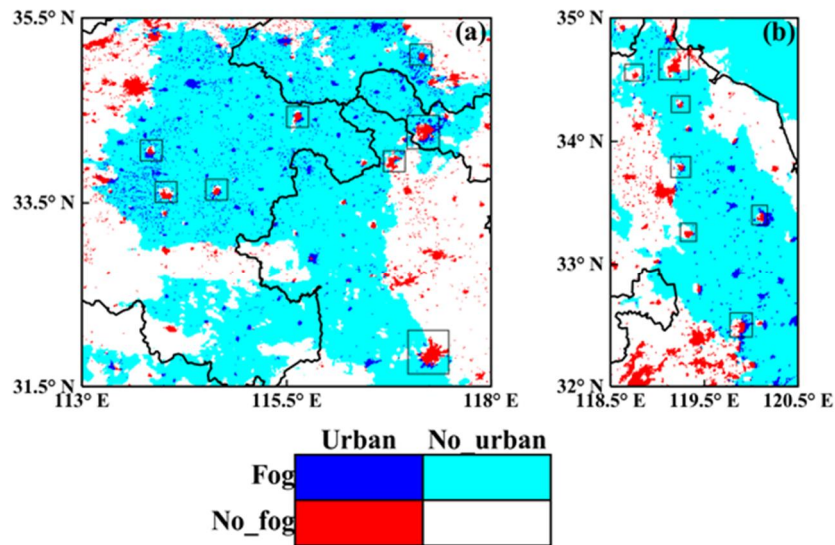


192

193 Figure 2. The performance of the simulated fog zone at 08:00 03 January 2017. (a) Himawari 8 RGB composite cloud  
194 image overlaid with the MICAPS observation sites (light red dots) at which fog was observed (relative humidity > 90 %  
195 and VIS < 1 km). (b) Simulated LWP distribution. Only LWC below 1500 m are integrated. The blue dots are the SX  
196 site. The two dashed rectangles in (a) are the subregions of interest in Fig. 3.

197

198 **Line 480-486 (Figure 3)**



199

200 Figure 3. Two sub-regions (a and b) with obvious fog holes on the Himawari 8 image at 11:00 03 January 2017. The  
201 fog zone, which is represented by albedo  $> 0.45$  (at  $0.64 \mu\text{m}$ ) and brightness temperature  $> 266 \text{ K}$  (at  $12.4 \mu\text{m}$ ) (Di Vit-  
202 torio et al., 2002), is marked with cold colours (blue or cyan). The urban areas are marked with blue or red. The red  
203 and white pixels surrounded or semi-surrounded by cold colours are fog holes, and among these pixels, the red pixels  
204 indicate the fog holes over urban areas. **Some of the cities with fog holes are marked by rectangles.**

205

206 **Replies to Referee#2**

207 We appreciate your valuable suggestions of our manuscript.

208

209 **Replies to Referee#3**

210 **1.** The focus of this study is on the radiative fog. However, there are different fog formation in atmosphere. For exam-  
211 ple, the advection fog formation is often occurred in the coast of eastern China. The Authors should highlight that un-  
212 der different fog conditions (i.e., radiative fog or advection fog, etc.) what is the effects of the urbanization and aerosol  
213 particles on the fog formation.

214 Thank you for this valuable suggestion. We agree that radiation fog and advection fog are two major fog types in Chi-  
215 na. They can occur in both inland and coastal areas. Gu et al. (2019) revealed the occurring frequencies of different fog  
216 types in Shanghai, a coastal city, during the past three decades. The major fog type is radiation fog (38.3%), followed  
217 by advection fog (27.7%) and advection-radiation fog (23.4%). Therefore, we infer that the dominant fog type in in-  
218 land areas and coastal areas is radiation fog, which should be attracted more attention.

219 Compared with radiation fog which usually occurs under stagnant weather conditions, advection fog is associated with  
220 synoptic forcing, i.e., advection of a moist air mass with contrasting temperature properties with respect to the underly-  
221 ing surface (Gultepe et al., 2007). The role of synoptic forcing should be considered when studying the effects of ur-  
222 banization and aerosols on advection fog, which is more complex than radiation fog. Zhong et al. (2017) indicated that  
223 urbanization and aerosols have nonsignificant effects on convective precipitation when the synoptic forcing is strong.  
224 Therefore, this study focuses on radiation fog to study the effects of urbanization and aerosols.

225 **References**

226 Gu, Y., Kusaka, H., van Doan, Q., and Tan, J.: Impacts of urban expansion on fog types in Shanghai, China: Numerical experiments by  
227 WRF model, *Atmos. Res.*, 220, 57–74, <https://doi.org/10.1016/j.atmosres.2018.12.026>, 2019.

228 Zhong, S., Qian, Y., Zhao, C., Leung, R., Wang, H., Yang, B., Fan, J., Yan, H., Yang, X., and Liu, D.: Urbanization-induced urban heat  
229 island and aerosol effects on climate extremes in the Yangtze River Delta region of China, *Atmos. Chem. Phys.*, 17, 5439–5457,  
230 <https://doi.org/10.5194/acp-17-5439-2017>, 2017.

231

232 **2. Is this study suitable for the most of large cities in eastern China?**

233 Thank you for this valuable suggestion. In the reply to comment1, we infer that the dominant fog type in inland areas  
234 and coastal areas of eastern China is radiation fog. Under the unified leadership of national government, most of the  
235 cities in eastern China experience the similar development pattern, i.e., the expansion of urban areas is commonly ac-  
236 companied by increasing aerosol pollution. So we believe our results of radiation fog are suitable for most of the cities  
237 in eastern China.

238

239 **3. Some important references are missing. For example, Tie et al (2017) studied the important feedback of atmospheric**  
240 **moister on the aerosol pollution in eastern China, which should state in the instruction.**

241 References

242 Tie, X., R.J. Huang, J.J. Cao, Q. Zhang, Y.F. Cheng, H. Su, D. Chang, U. Pöschl, T. Hoffmann, U. Dusek, G. H. Li, D. R. Worsnop, C. D.  
243 O'Dowd, Severe Pollution in China Amplified by Atmospheric Moisture, Sci. Rep. 7: 15760 DOI:10.1038/s41598-017-15909-1, 2017.

244 Tie, XX, X. Long, GH Li, SY Zhao, JJ Cao, JM Xu, Ozone enhancement due to photo-dissociation of nitrous acid in eastern China, Atmos.  
245 Chem. Phys., 19,11267–11278, 2019.

246 Thank you for this valuable suggestion. We have added the two references and some texts.

247 **Line 53-54 (Introduction)**

248 Aerosols exert sophisticated impacts on fog through direct (radiation) effects and indirect (microphysical) effects  
249 (Khain and Pinsky, 2018). **Aerosols attenuate shortwave radiation, influencing PBL structure and the vertical pro-**  
250 **file of moisture and aerosols (Tie et al., 2017, 2019), which can alter the formation and dissipation condition of**  
251 **fog....**

# To what extents do urbanization and air pollution affect fog?

Shuqi Yan<sup>1,2,3,4</sup>, Bin Zhu<sup>1,2,3,4,\*</sup>, Yong Huang<sup>5,6</sup>, Jun Zhu<sup>7</sup>, Hanqing Kang<sup>1,2,3,4</sup>, Chunsong Lu<sup>1,2,3,4</sup>, Tong Zhu<sup>8</sup>

<sup>1</sup>Collaborative Innovation Center on Forecast and Evaluation of Meteorological Disasters, Nanjing University of Information Science & Technology, Nanjing, China

<sup>2</sup>Key Laboratory for Aerosol-Cloud-Precipitation of China Meteorological Administration, Nanjing University of Information Science & Technology, Nanjing, China

<sup>3</sup>Key Laboratory of Meteorological Disaster, Ministry of Education (KLME), Nanjing University of Information Science & Technology, Nanjing, China

<sup>4</sup>Special test field of National Integrated meteorological observation, Nanjing University of Information Science & Technology, Nanjing, China

<sup>5</sup>Anhui Meteorology Institute, Key Lab of Atmospheric Science and Remote Sensing Anhui Province, Hefei 230031, China

<sup>6</sup>Shouxian National Climatology Observatory, Shouxian 232200, China

<sup>7</sup>Xiangshan Meteorological Bureau, Xiangshan 315700, China

<sup>8</sup>IMSG at NOAA/NESDIS/STAR, 5830 University Research Ct., College Park, MD 20740, USA

*Correspondence to:* Bin Zhu (binzhu@nuist.edu.cn)

**Abstract.** The remarkable development of China has resulted in rapid urbanization (urban heat island and dry island) and severe air pollution (aerosol pollution). Previous studies demonstrate that these two factors have either suppressing or promoting effects on fog, but what are the extents of their individual and combined effects? In this study, a dense radiation fog event in East China in January 2017 was reproduced by the WRF-Chem model, and the individual and combined effects of urbanization and aerosols on fog (indicated by liquid water content (LWC)) are quantitatively revealed. Results show that urbanization inhibits low-level fog, delays its formation and advances its dissipation due to higher temperatures and lower saturations. In contrast, upper-level fog could be enhanced because of the updraft-induced vapour convergence. Aerosols promote fog by increasing LWC, increasing droplet concentration and decreasing droplet effective radius. Further experiments show that the current pollution level in China ~~is~~ **could be** still below the critical aerosol concentration that suppresses fog. Urbanization influences fog to a larger extent than do aerosols. When urbanization and aerosol pollution are combined, the much weaker aerosol promoting effect is counteracted by the stronger urbanization suppressing effect on fog. Budget analysis of LWC reveals that urban development (urbanization and aerosols) alters LWC profile and fog structure mainly by modulating condensation/evaporation process. Our results infer that urban fog will be further reduced if urbanization keeps developing and air quality keeps deteriorating in the future.

## 31 1 Introduction

32 During the past five decades, China has achieved remarkable developments, accompanied by strong anthropogenic activities  
33 (rapid urbanization and severe air pollution). Urbanization and air pollution have significantly affected climate change,  
34 monsoons, air quality, fog, clouds and precipitation (e.g., Li et al., 2016; Li et al., 2017). Many-Previous studies have linked  
35 the changes in clouds and precipitation to urbanization and aerosols. Urbanization destabilizes the boundary layer, which  
36 triggers strong updrafts and invigorates convection (e.g., Rozoff et al., 2003; Shepherd, 2005). Aerosols modify the macro-  
37 scopic, microphysics, thermodynamics and radiative properties of clouds through complicated pathways, which are called as  
38 aerosol-cloud-radiationaerosol-radiation and aerosol-cloud interactions and have been systematically reviewed by Fan et al.  
39 (2016), Rosenfeld et al. (2014), Tao et al. (2012), etc. Fog can be viewed as a cloud (Leng et al., 2014) that occurs near the  
40 surface. Land use features and aerosol properties may instantly affect fog, so fog is more sensitive to anthropogenic activities  
41 than other types of clouds are (Zhu and Guo, 2016). Many-Previous studies have analysed the effects of urbanization and  
42 aerosols on fog, mostly in segregated manners.

43 Urbanization is featured with urban heat island (UHI) and dry island (UDI) effects. The urban surface has a lower albedo,  
44 which reduces the reflected solar radiation and enhances heat storage. Urban expansion decreases the coverage of cropland,  
45 water bodies and forestland, which reduces the sources of water vapour. As a result, urban areas commonly experience high-  
46 er temperatures and lower vapour contents. These conditions induce a lower relative humidity supersaturation that is unfavourable  
47 for fog formation (Gu et al., 2019). In the long-term scale, urban fog days are reported to decrease significantly  
48 (e.g., Guo et al., 2016; LaDochy, 2005; Sachweh and Koepke, 1995; Shi et al., 2008; Yan et al., 2019). Although UHI and  
49 UDI inhibit near-surface fog, the upward motions can promote upper-level fog (Li et al., 2011; Niu et al., 2010b). Surface  
50 roughness and thermal circulation cause strong updrafts (Rozoff et al., 2003), which transfer water vapour aloft and cause  
51 wet island phenomenon in the upper-level (Kang et al., 2014). The fog at that altitude may be subsequently enhanced.

52 Aerosols exert sophisticated impacts on fog through direct (radiation) effects and indirect (microphysical) effects (Khain and  
53 Pinsky, 2018). Aerosols attenuate shortwave radiation, influencing PBL structure and the vertical profile of moisture and  
54 aerosols (Tie et al., 2017, 2019), which can alter the formation and dissipation condition of fog. Scattering aerosols block  
55 downwelling solar radiation in the daytime, thus delaying the dissipation and elongating the duration of fog (Shi et al., 2008;  
56 Maalick et al., 2016). Although they increase downwelling longwave radiation at night, scattering aerosols have negligible  
57 effects on the fog formation time (Stolaki et al., 2015; Maalick et al., 2016). The role of absorbing aerosols like BC on fog  
58 depends on its residence height. If BC resides above the fog layer, BC causes a dome effect (Ding et al., 2016) which blocks  
59 solar radiation and prevents the dissipation of fog (Bott, 1991). If BC resides within the fog layer, BC heats fog droplets and  
60 accelerates the dissipation of fog (Maalick et al., 2016). The aerosol indirect effect on cloud is addressed as one of the most

批注 [yansq1]: Referee#1\_Comment2

批注 [yansq2]: Referee#1\_Comment1

批注 [yansq3]: Referee#1\_Comment2

批注 [yansq4]: Referee#1\_Comment3

批注 [yansq5]: Referee#3\_Comment3

61 uncertain factors in the IPCC report (IPCC, 2013). Aerosol concentration has a two-fold effect on fog, which is called as the  
62 boomerang pattern (Koren et al., 2008). Under saturation conditions, increasing aerosols commonly result in more CCNs. It  
63 promotes activation and condensation, yielding more but smaller droplets and increasing cloud water content (Fan et al.,  
64 2018; Rosenfeld et al., 2008). These changes have two kinds of positive feedback on fog (Maalick et al., 2016): more drop-  
65 lets cause stronger radiative cooling at fog top and enhance condensation (Jia et al., 2018); smaller droplet size inhibits sed-  
66 imentation and the depletion of cloud water (Zhang et al., 2014). However, if aerosol concentration exceeds a certain thresh-  
67 old, this promoting effect disappears (Quan et al., 2011) or even turns into a suppressing effect due to the strong vapour  
68 competition (Guo et al., 2017; Koren et al., 2008; Liu et al., 2019; Rangognio, 2009; Wang et al., 2015). Additionally,  
69 large-scale aerosol pollution can change weather patterns and affect large-scale fog formation conditions (Niu et al., 2010a).  
70 Ding et al. (2019) found that the dome effects of BC induce a land-sea thermal contrast and generate a cyclonic anomaly  
71 over coastal areas. This anomaly results in more vapor transported inland and strengthened advection-radiation fog.

批注 [yansq6]: Referee#1\_Comment4

72 ~~Our recent observational work (Yan et al., 2019) indicated a decreasing trend in fog days, and Yan et al. (2019) analysed de-~~  
73 ~~cadal trends of fog days and quantitatively proved that~~ the inhibiting effects of urbanization outweigh the promoting effects  
74 of aerosols on fog during the mature urbanization stage. ~~Their study inspires us~~ This study aims to quantitatively ~~confirm~~  
75 ~~confirm~~ the roles of urbanization and aerosols in a dense fog event by an online-coupled synoptic and air quality model,  
76 WRF-Chem. This event is a radiation fog event with weak synoptic forcing (detailed in Sect. 3.1), so the effects of urbaniza-  
77 tion and aerosols should be obvious. Determining the quantitative extents of urbanization effect, aerosol effect and their  
78 combined effect is an interesting topic, which has barely been studied previously to the best of our knowledge. This work ~~is~~  
79 ~~expected to~~ facilitates the understanding of how anthropogenic activities affect the natural environment, fog (cloud) physics  
80 and aerosol-cloud interactions near the surface.

批注 [yansq7]: Referee#1\_Comment5

批注 [yansq8]: Referee#1\_Comment6

81 In this study, urbanization mainly refers to UHI and UDI associated with land use change and human activities, excluding the  
82 increasing aerosol pollution caused by urban expansion. Air pollution refers to aerosols and is indicated by anthropogenic  
83 emissions because aerosol concentration is highly proportional to emission intensity. Liquid water content (LWC) and  
84 cloud/fog droplet number concentration ( $N_d$ ) are two important parameters representing fog intensity and visibility. Follow-  
85 ing previous studies (e.g., Ding et al., 2019; Gu et al., 2019; Jia et al., 2018; Maalick et al., 2016; Yang et al., 2018), we use  
86 LWC as the indicator of fog to reveal different characteristics of fog in different experiments. This study is organized as fol-  
87 lows. The data, model and methods are described in Sect. 2. Section 3.1 overviews the fog event and provides preliminary  
88 evidence of how urban development affects fog. Section 3.2 evaluates the model performance. Sections 3.3 to 3.5 analyse the  
89 urbanization, aerosol and combined effects on fog. Section 3.6 discusses the rationality and reliability of the results. ~~Section~~  
90 ~~4 concludes the findings of this study.~~

批注 [yansq9]: Referee#1\_Comment7

## 91 2 Data, model and methods

### 92 2.1 Data

93 The first data are the hourly automatic weather station data from the Shouxian National Climate Observatory (SX; 32.4° N,  
94 116.8° E, 23 m) that are used to evaluate the model performance. SX is a rural site surrounded by vast croplands and is ap-  
95 proximately 30 km away from the nearest large city, [Huainan](#) (Fig. 1b). The data include horizontal visibility, temperature,  
96 relative humidity, wind direction and speed. The second data are the Himawari 8 satellite data that are used to represent fog  
97 area (<https://www.eorc.jaxa.jp/tree/index.html>). Fog area is mainly indicated by the albedo at three visible bands: red (band  
98 3, 0.64  $\mu\text{m}$ ), green (band 2, 0.51  $\mu\text{m}$ ) and blue (band 1, 0.47  $\mu\text{m}$ ). The third data are the 3-hourly data from the Meteorologi-  
99 cal Information Comprehensive Analysis and Process System (MICAPS) (Li et al., 2010) that are also used to represent the  
100 fog area. The fourth data are the land use data from the Moderate Resolution Imaging Spectroradiometer Land Cover Type  
101 Version 6 data (MCD12Q1; <https://lpdaac.usgs.gov/products/mcd12q1v006>) in the year of 2017, the same as the simulation  
102 period. The data are resampled from 500 m to 30 arc-seconds (approximately 1 km) and [used to](#) replace the geological data  
103 of the WRF model.

批注 [yansq10]: Refer-  
ee#1\_Comment8

### 104 2.2 Model configuration

105 The model used in this study is the WRF-Chem (V3.9.1.1) model. It is an online-coupled mesoscale synoptic and air quality  
106 model that considers the sophisticated interactions among various dynamic, physical and chemical processes (Chapman et al.,  
107 2009; Fast et al., 2006). WRF or WRF-Chem has been successfully used in simulating fog events (Jia and Guo, 2012; Jia and  
108 Guo, 2015; Jia et al., 2018) and exploring aerosol-cloud interactions (Fan et al., 2018). Two nest domains are set up (Fig. 1).  
109 The d01 domain has a size of 217 $\times$ 223 grids and a resolution of 6 km, covering the entire fog area of this event (Fig. 2a).  
110 The d02 domain has a size of 115 $\times$ 121 grids and a resolution of 2 km, covering SX and the adjacent areas. The land use data  
111 are replaced by MCD12Q1 data, which represent the latest condition.

112 Fog simulation is highly sensitive to vertical grids (Gultepe et al., 2007). A fine vertical resolution with a proper lowest  
113 model level can better resolve turbulences, thus yielding a reasonable fog structure (Yang et al., 2019). Here, 42 vertical lev-  
114 els are established with the first five  $\eta$  values of 1.000, 0.999, 0.998, 0.997, 0.996. There are 25 levels below the boundary  
115 layer (approximately 1500 m), and the lowest model level is approximately 8 m.

116 Fog simulation is also sensitive to physical schemes (Gu et al., 2019). Through numerous experiments, radiation, micro-  
117 physics and boundary schemes are found to significantly influence the model performance, and the boundary layer scheme  
118 plays a decisive role (Naira Chaouch et al., 2017). The radiation schemes are the RRTM longwave scheme and the Goddard

批注 [yansq11]: Refer-  
ee#1\_Comment9



119 shortwave scheme. The microphysical scheme is the Morrison double-moment scheme (Morrison et al., 2005). The boundary  
120 layer scheme is the YSU 1.5-order closure non-local scheme, which yields better results than do any other schemes. The  
121 major schemes are listed in Tab. 1.

122 The model is driven by the highest resolution product (0.125°, approximately 13 km) of ECMWF data  
123 (<https://apps.ecmwf.int/datasets/data/interim-full-daily/levtype=sfc/>). The anthropogenic emissions are derived from the  
124 Multi-resolution Emission Inventory for China (MEIC) database (<http://www.meicmodel.org>). The simulation starts at  
125 2017-01-01 08:00 and ends at 2017-01-03 14:00, with the first 24 hours as the spin-up period (all the times here are in local  
126 time).

### 127 **2.3 Sensitivity experiments**

128 The study site is SX because only its visibility is observed hourly and is a multiple of 1 m, which is suitable for evaluating  
129 the model performance. To investigate the effects of urbanization and aerosols on fog, we change the land use and emission  
130 intensity around SX. Four experiments, i.e., u0e0, u3e0, u0e3 and u3e3 are designed. The u0e0 is the base experiment, with  
131 no urbanization and weak emission at SX. The u3e0 is set as the urbanization condition. The u0e3 is set as the polluted con-  
132 dition. The u3e3 is set as the urban development condition (urbanization and pollution coexist). The experiment settings are  
133 listed in Tab. 2.

134 On the setting of urbanized condition, we replace the land use of SX as that of Hefei, the most urbanized city and the capital  
135 of Anhui Province. The downtown of Hefei has a built area of approximately 570 km<sup>2</sup>. Therefore, the 11x13 box centered on  
136 SX (572 km<sup>2</sup>) is replaced by urban surface in the u3e0 and u3e3 experiments to represent the urbanization condition.

137 The downtown of Hefei has much higher emissions than SX. For example, the PM<sub>2.5</sub> emission rate of Hefei is 40 times  
138 higher than that of SX. To represent the polluted condition, the emission intensity of the aforementioned box is set to be  
139 equal to that of downtown Hefei in the u0e3 and u3e3 experiments.

### 140 **2.4 Calculating visibility**

141 The LWC is the proxy of fog as mentioned above. Since the LWC is not observed, and visibility (VIS) is related to LWC, the  
142 VIS is used to assess the model performance. VIS is not diagnosed by the model and can be parameterized by the function of  
143 LWC, N<sub>d</sub> or droplet effective radius (R<sub>e</sub>). Equation 1 (Kunkel, 1983) and 2 (Gultepe et al, 2006) are two parameterization  
144 methods.

$$\text{VIS}[\text{m}] = 27\text{LWC}[\text{g cm}^{-3}]^{-0.88} \quad (1)$$

$$\text{VIS}[\text{m}] = 1002(\text{LWC}[\text{g cm}^{-3}] \cdot \text{N}_d[\text{cm}^{-3}])^{-0.6473} \quad (2)$$

145 Another parameterization method is based on the Mie theory (Gultepe et al., 2017). VIS is inverse proportional to atmos-  
 146 pheric extinction at visible wavelength. The extinction coefficient of cloud water ( $\beta_c$ ) is

$$\beta_c [\text{km}^{-1}] = \frac{3Q_{ext} \rho_a \text{LWC}}{4\rho_w R_c} \times 10^6 \quad (3)$$

147 where  $\rho_a$  ( $\rho_w$ ) is the air (water) density in  $\text{kg m}^{-3}$ , LWC is in  $\text{g kg}^{-1}$ ,  $R_c$  is in  $\mu\text{m}$ , and  $Q_{ext}$  is the extinction efficiency, which is  
 148 assumed to be 2 for cloud droplets.

149 The atmospheric extinction ( $\beta$ ) is also largely contributed by aerosols ( $\beta_a$ ) and other types of hydrometeors. The model diag-  
 150 noses  $\beta_a$  at 550 nm. No other types of hydrometeors occur in this fog case, so we assume  $\beta = \beta_a + \beta_c$ . Then VIS is determined  
 151 by the Koschmieder rule (Koschmieder, 1924):  $\text{VIS}[\text{m}] = 3.912/\beta[\text{km}^{-1}] \times 1000$ .

152 During fog period (Fig. 4 shaded zone), the three methods nearly yield the same results (figure not shown), so the last meth-  
 153 od is used to calculate the simulated VIS.

## 154 **3 Results and discussions**

### 155 **3.1 Overview of the fog event**

#### 156 **3.1.1 Formation condition and lifetime**

157 From 01 to 06 January 2017, East China is dominated by zonal circulation, with weak trough, ridge, pressure gradient and  
 158 atmospheric diffusion (Zhang and Ma, 2017). Under this stable weather pattern, the accumulation of pollutants and water  
 159 vapour promote the occurrence of fog-haze events. From the evening of 02 January to the noon of 03 January, a dense fog  
 160 event occurs in wide regions of East China. The fog reaches its peak at 08:00 03 January, covering south Hebei, east Henan,  
 161 west Shandong, Anhui, Jiangsu and Shanghai (Fig. 2a). Figure 4a shows the temporal variation of visibility at SX. The fog  
 162 forms at 18:00 02 January and dissipates at 12:40 03 January. This is a radiation fog which is promoted by strong radiative  
 163 cooling at night and weak easterly water vapour transport from northwest Pacific (Zhu et al., 2019).

#### 164 **3.1.2 Preliminary evidence of urban development affecting fog**

165 Lee (1987) and Sachweh and Koepke (1995) observed "fog holes" over urban areas on satellite images. Here, fog hole means

166 the low liquid water path (LWP) region within the fog region, which is visualized as pixels with weak fog (high visibility) or  
167 clear sky surrounded by dense fog. These holes demonstrate that urban development (urbanization and aerosols) has a clear-  
168 ing effect on fog. In this fog event, fog holes are also present over urban areas on the Himawari 8 image at 11:00 03 January  
169 (Fig. 3). We assume that ~~urbanization and air pollution~~ could have profound effects on fog by reducing the LWP or advanc-  
170 ing the dissipation of fog, and the role of aerosols on fog is weaker than that of urbanization.

批注 [yansq12]: Refer-  
ee#1\_Comment10

## 171 3.2 Model evaluation and simulations

172 The model performance is evaluated by comparing the fog spatial coverage. Satellite cloud image and modelled LWP ( $>2 \text{ g}$   
173  $\text{m}^{-3}$ ) can represent the observed and simulated fog zone, respectively (Jia et al., 2018). Figure 2 shows the Himawari 8 visible  
174 cloud image and the simulated LWP distribution at 08:00. The light white pixels and light red dots indicate the observed fog  
175 area. The model well captures the fog in south Hebei, east Henan, west Shandong, Anhui, Jiangsu and Shanghai.

批注 [yansq13]: Refer-  
ee#1\_Comment11

176 The model performance is also evaluated by comparing the visibility and other basic parameters at the SX site (Fig. 4). Seen  
177 from the visibility, the simulated fog forms at 19:30, 1.5 h later than the observation, and dissipates at 12:20, 30 min earlier  
178 than the observation. During the fog period, the simulated visibility agrees well with the observation. The other parameters  
179 such as temperature, wind speed and relative humidity are also effectively reproduced by the model, with relative small  
180 RMSEs of 0.8 K, 0.7 m/s and 5.9 %, respectively. Overall, the model well captures the spatial feature and temporal evolution  
181 of the fog.

## 182 3.3 Urbanization effects

183 From different sensitivity experiments (u3e0, u0e3 and u3e3), we can deduce the extents of the separate or combined effects  
184 of urbanization and aerosols on fog. Figure 5 compares the LWC between u0e0 and u3e0. The general results are: (1) Before  
185 02:00, urbanization leads to a decreasing LWC in all layers. Fog forms on the surface at 22:30 in u3e0, 3 h later than in u0e0.  
186 (2) After 02:00, the LWC decreases in the low-level while it increases in the upper-level. Fog dissipates at 10:50 in u3e0, 1.5  
187 h earlier than in u0e0. To better explain the LWC difference, its profiles are shown in Fig. 6. At 23:00, although fog has  
188 formed in u3e0, the fog is rather weak compared with u0e0, which is caused by the higher temperature (Fig. 6f) and lower  
189 saturation associated with UHI and UDI. At 02:00, fog develops in u3e0, but its intensity (the value of LWC) cannot reach  
190 the same level as that in u0e0.

191 An interesting phenomenon is the opposite change of LWC in the low-level and upper-level after 02:00. This phenomenon  
192 can be explained by the role of updrafts. The increasing roughness length and extra warming in urban conditions could trig-  
193 ger horizontal wind convergence (Fig. S1) and the enhanced updrafts (Fig. 5c). The stronger updrafts in u3e0 affect conden-

194 sation via two possible pathways: (1) the vertical transport of vapour ( $-w \frac{\partial q}{\partial z}$ ) and vertical convergence/divergence ( $-q \frac{\partial w}{\partial z}$ ) re-  
195 distribute water vapour and affect condensation; (2) the adiabatic cooling promotes condensation. The role of the first path-  
196 way is measured by vertical vapour flux divergence ( $\frac{1}{g} \frac{\partial(qw)}{\partial z}$ ). At 05:00, u3e0 shows a stronger vapour convergence above 110  
197 m (Fig. 6h), and the LWC increases above 130 m (Fig. 6c). At 08:00, u3e0 shows a stronger vapour convergence above 130  
198 m (Fig. 6i), and the LWC increases above 170 m (Fig. 6d). Therefore, it is possible that the adiabatic cooling and up-  
199 draft-induced vapour flux convergence increase the vapour content and promote condensation in the upper-level, while the  
200 fog in the low-level is suppressed by the divergence of vapour flux. At 11:00, fog disappears at the ground in u3e0 likely due  
201 to the higher temperature (Fig. 6j). In summary, the UHI, UDI and updrafts alter the profile of LWC and reduce the LWP  
202 most of the time (Fig. 5c), and the decreasing LWP in the daytime can explain why fog holes occur above urban areas (Fig.  
203 3).

### 204 3.4 Aerosol effects

205 Figure 7 compares the LWC between u0e0 and u0e3. The formation time, dissipation time of fog and fog top show almost no  
206 changes. The LWC increases at almost all layers in the polluted condition. Accordingly, the LWP also increases (Fig. 7c). It  
207 is probable that the current pollution level of China always promotes fog occurrence. To testify whether the u0e3 is below  
208 the transition point of the boomerang pattern, eight additional experiments (D10, D7.5, D5, D2.5, M2.5, M5, M7.5 and M10)  
209 are performed. These experiments are the same as u0e3, except that the emissions around SX (the black box in Fig. 1b) are  
210 multiplied (the "M" prefix) or divided (the "D" prefix). For example, the name M2.5 means multiplying by 2.5 ~~times~~; the  
211 name D10 means dividing by 10 ~~times~~.

212 Figure 8 compares the LWC,  $N_d$ ,  $R_e$  and LWP among the nine emission-variant experiments. All the four parameters show  
213 the boomerang pattern, which demonstrates that the model is able to simulate the dual effects of aerosols. Below u0e3, the  
214 four parameters monotonically vary with emission level or CCN concentration, indicating that aerosol pollution could al-  
215 ways promote fog. This phenomenon is because stronger emissions produce more aerosols and CCN. Under saturation con-  
216 ditions, the larger amount of CCN boost activation and yield a higher  $N_d$ . The higher  $N_d$  reduces  $R_e$  and inhibits autoconver-  
217 sion and sedimentation (Twomey, 1977); thus, this situation decreases the depletion of fog water and increases the LWC.  
218 This promoting effect has been confirmed by ~~many previous~~ model studies (e.g., Maalick et al., 2016; Stolaki et al., 2015)  
219 and observations (e.g., Chen et al., 2012; Goren and Rosenfeld, 2012). The ~~aerosol-CCN<sub>0.1</sub>~~ concentration of u0e3 ( $570 \text{ cm}^{-3}$ )  
220 is lower than that of the turning point (experiment M2.5) ( $1349 \text{ cm}^{-3}$ ) is higher than that of u0e3 (Fig. 8), revealing possibly  
221 indicating that the current pollution level in China (u0e3) is still located in the promoting regime rather than the suppressing  
222 regime of fog occurrence, ~~which is also found by Jia et al. (2018)~~.

批注 [yansq14]: Refer-  
ee#1\_Comment14

批注 [yansq15]: Refer-  
ee#1\_Comment2

Rosenfeld et al. (2008) revealed that the turning point of boomerang pattern in convective clouds is  $CCN_{0.4} = 1200 \text{ cm}^{-3}$ . The  $CCN_{0.4}$  of u0e3 is  $6023 \text{ cm}^{-3}$ , which seems to suppress fog. Aerosols affect convective clouds through two competing mechanisms: 1) invigorating convection by promoting vapour condensation. 2) suppressing convection by blocking solar radiation and reducing surface heat flux. Under polluted conditions ( $AOD > 0.3$  or  $CCN_{0.4} > 1200 \text{ cm}^{-3}$ ), the suppressing effect outweighs the invigoration effect, so the turning point occurs (Koren et al., 2008; Rosenfeld et al., 2008). This suppressing effect does not exist in fog because fog commonly formed at night. Therefore, the turning point in fog might occur later than that in convective clouds. In North China Plain where air pollution is thought to be more serious, a case study by WRF-Chem also indicates that fog properties (e.g., LWC,  $N_d$  and LWP) increase monotonically when emission intensity varies from 0.05-fold to 1-fold.

批注 [yansq16]: Reference#1\_Comment13

### 3.5 Combined effects of urbanization and aerosols

Figure 9 compares the LWC between u0e0 and u3e3. The u3e3-induced change is quite similar to but not the same as the u3e0-induced change. The time-height average of absolute change of LWC induced by u3e0, u0e3 and u3e3 are  $0.120$ ,  $0.019$ ,  $0.124 \text{ g kg}^{-1}$ , respectively. This result indicates that urbanization affects fog to a larger extent than do aerosols; when urbanization and aerosols are combined, the effect of aerosols is indiscernible. The LWP is also significantly suppressed in the daytime, and the promoting effect of aerosols in Fig. 7c is indiscernible in Fig. 9c. To further explain the changes in LWC, we perform budget analysis of the LWC to determine which physical processes are the dominant contributors.

In WRF, the budget of LWC is composed of the following items,

$$\frac{\partial q_c}{\partial t} = - \underbrace{\left( u \frac{\partial}{\partial x} + v \frac{\partial}{\partial y} + w \frac{\partial}{\partial z} \right) q_c}_{\text{adv}} + \left( \frac{\partial q_c}{\partial t} \right)_{\text{PBL}} + \left( \frac{\partial q_c}{\partial t} \right)_{\text{micro}} + \left( \frac{\partial q_c}{\partial t} \right)_{\text{cumu}} \quad (4)$$

where  $q_c$  is LWC, and the subscripts denote advection, boundary layer, microphysical and cumulus processes, respectively.

The microphysical tendency is further decomposed into the following items,

$$\left( \frac{\partial q_c}{\partial t} \right)_{\text{micro}} = \left( \frac{\partial q_c}{\partial t} \right)_{\text{cold}} + \left( \frac{\partial q_c}{\partial t} \right)_{\text{auto}} + \left( \frac{\partial q_c}{\partial t} \right)_{\text{accr}} + \left( \frac{\partial q_c}{\partial t} \right)_{\text{sedi}} + \left( \frac{\partial q_c}{\partial t} \right)_{\text{cond/evap}} \quad (5)$$

where the subscripts denote cold phase processes, autoconversion, accretion, sedimentation and condensation/evaporation, respectively.

All the processes regarding precipitation and cold phase (the cumu, cold, auto and accr subscripts) are not analysed because

245 no precipitation occurs, and the temperature is above 0°C in the simulated fog (figure not shown). The sum of microphysical  
246 (condensation/evaporation and sedimentation), boundary layer and advection tendencies is equal to the LWC distribution, so  
247 the contributions of other physical processes can be safely ignored.

248 We can also infer that to what extents the various physical processes affect fog through the sensitivity experiments (u3e0,  
249 u0e3 and u3e3). Additional aerosols weakly influence these processes (Fig. S2 right column) and subsequently result in weak  
250 LWC change (Fig. 7c). Compared with aerosols, urbanization effect is much more considerable (Fig. S3 right column); it  
251 dominantly accounts for the variation in physical tendencies from u0e0 to u3e3 (Fig. 10 right column). In u3e3 condition,  
252 urban development (urbanization and aerosols) induces different magnitude of changes in different physical tendencies. The  
253 relative magnitudes are 52.1, 38.3 and 9.6 % for the microphysical, boundary layer and advection processes, respectively,  
254 indicating that microphysics is most susceptible to urban development and contributes most to the LWC change. Among  
255 various microphysical processes, condensation/evaporation contributes most (72.7 %) to the change in microphysical ten-  
256 dency (Fig. 11 right column). The above results indicate that urban development affects the LWC mainly by modulating the  
257 condensation/evaporation process. Since u3e3 condition still witnesses higher temperatures and stronger updrafts (figure not  
258 shown), the notable variation in condensation/evaporation tendency induced by u3e3 can also be attributed to the predomi-  
259 nant role of UHI, UDI and updrafts. The mechanism has been analysed in Sect. 3.3.

### 260 **3.6 Discussions**

261 As mentioned above, urbanization influences fog to a larger extent than do aerosols; the LWC in fog does not vary substan-  
262 tially with pollution level. This section discusses the rationality and reliability of our results through mechanism analysis and  
263 observational evidence.

264 The sensitivity of cloud properties to aerosols depends on aerosol concentration and saturation environment. In convective  
265 clouds with intense upward motions and high saturations, the response of cloud properties to additional aerosols is signifi-  
266 cant ("aerosol-limited regime") (Fan et al., 2018). However, in fog with much weaker updrafts and lower saturations, this  
267 response could be more sensitive to vapour content rather than aerosol concentration ("vapour-limited regime"). It possibly  
268 implies that the LWC in fog varies slightly with pollution level but considerably with saturation condition that related to ur-  
269 banization. Our results reveal that the time-height average LWC varies within the extent of 0.07g kg<sup>-1</sup> when emission inten-  
270 sity varies within two orders of magnitude (Fig. 8). This relative weak response of the LWC to pollution level is also report-  
271 ed by Jia et al. (2018).

272 In terms of observational evidence, Yan et al. (2019) revealed that fog days in polluted regions of East China have decreased  
273 since the 1990s. Through quantitative analysis, the promoting effects of aerosols are weakening, while the suppressing ef-

274 fects of urbanization are enhancing and dominantly cause this decrease. Sachweh and Koepke (1995) also claimed that the  
275 hindering effects of urbanization outweigh the promoting effects of aerosols on fog in southern Germany. Additionally, satel-  
276 lite images present discernible fog holes above urban areas (Fig. 3) (Lee, 1987; Sachweh and Koepke, 1995). Therefore,  
277 these observational evidence support the model results that the promoting effect of aerosols is counteracted by the hindering  
278 effect of urbanization. We believe that the results can also be applied to other [large](#) cities in China because these cities com-  
279 monly witness strong UHI, UDI and severe air pollution.

## 280 4 Conclusions

281 A dense radiation fog event occurred in East China from 02 to 03 January 2017. Satellite images show that fog holes occur  
282 over urban areas, demonstrating the remarkable effects of urbanization and air pollution on fog. Hence, the mechanism is  
283 investigated by the WRF-Chem model. The model well captures the spatial coverage and temporal evolution of the fog. Fur-  
284 thermore, the separate and combined effects of urbanization (refers to UHI and UDI) and air pollution (refers to aerosols) on  
285 fog (indicated by the LWC) are revealed, and the extents of these effects are quantitatively determined. Results show that:

286 Urbanization redistributes the LWC profile by the UHI, UDI effect and updrafts. The updrafts may be caused by surface  
287 roughness and extra warming. The UHI and UDI suppress low-level fog, delay its formation by 3 h, and advance its dissipa-  
288 tion by 1.5 h. However, the upper-level fog could be enhanced due to the updraft-induced adiabatic cooling and vapour flux  
289 convergence. Urbanization reduces the LWP most of the time, and this reduction in the daytime can explain why fog holes  
290 are present above urban areas on satellite images.

291 Aerosols promote fog mainly by changing microphysical properties. The increasing emissions (aerosol concentration) pro-  
292 duce more CCN and fog droplets, which decreases  $R_c$  and inhibits sedimentation, thus leading to a higher LWC. Further sen-  
293 sitivity experiments show that the current pollution level in China [is-could be](#) still below the transition point of the boomer-  
294 ang pattern that suppresses fog. The macroscopic properties such as fog top and lifetime remain nearly unchanged.

295 The role of urbanization far overweighs that of aerosols. Therefore, when they act together, the urbanization effect is domi-  
296 nant, and the aerosol effect is indiscernible. Budget analysis of LWC shows that increasing aerosols influence various physi-  
297 cal processes to a lesser extent, while urbanization influences these processes to a larger extent, eventually leading to a sub-  
298 stantial LWC change in urban development condition (urbanization and aerosols). In this condition, [the](#) comparisons among  
299 various physical processes reveal that microphysics dominates the change in LWC, and condensation/evaporation dominates  
300 the change in microphysical tendency. This result highlights the importance of condensation/evaporation process in modu-  
301 lating the LWC profile and fog structure.

302 Mechanism analysis and the observational evidence support our key finding that urbanization influences fog to a much larger  
303 extent than do aerosol pollution. Therefore, we believe our results are reasonable and robust in radiation fog events without  
304 strong synoptic forcings, and the results can also be applied to other [large](#) cities in China due to the similar urban develop-  
305 ment patterns. This study **is expected to** facilitate a better understanding of how anthropogenic activities affect the natural  
306 environment, fog (cloud) physics and aerosol-cloud interactions near the surface. We can also infer the future change of fog  
307 occurrence. Under the traditional urban development pattern, i.e., urbanization keeps developing and air quality keeps dete-  
308 riorating, urban fog occurrence will be further reduced.

309

310 *Code and data availability.* Some of the data repositories have been listed in Sect. 2. The other data, model outputs and  
311 codes can be accessed by contacting Bin Zhu via [binzhu@nuist.edu.cn](mailto:binzhu@nuist.edu.cn).

312

313 *Author contributions.* SY performed the model simulation, data analysis and manuscript writing. BZ proposed the idea, su-  
314 pervised this work and revised the manuscript. YH provided the observation data at the SX site. JZ processed the observation  
315 data. HK offered helps to the model simulation. CL and TZ also contributed to the manuscript revision.

316

317 *Competing interests.* The authors declare that they have no conflict of interest.

318

319 *Acknowledgments.* We are grateful to the High Performance Computing Center of Nanjing University of Information Science  
320 and Technology for doing the numerical calculations in this work on its blade cluster system. We thank American Journal  
321 Experts (AJE) for the English language editing.

322

323 *Financial support.* This work is supported by the National Key Research and Development Program (2016YFA0602003)  
324 and the National Natural Science Foundation of China (91544229, 41575148, 41605091).

## 325 **References**

326 Abdul-Razzak, H. and Ghan, S. J.: A parameterization of aerosol activation 3. Sectional representation, *J. Geophys. Res.*, 107,  
327 AAC-1-AAC 1-6, <https://doi.org/10.1029/2001jd000483>, 2002.

批注 [yansq17]: Refer-  
ee#1\_Comment6



328 Bott, A.: On the influence of the physico-chemical properties of aerosols on the life cycle of radiation fogs, *J. Aerosol. Sci.*, 21, 1–31,  
329 <https://doi.org/10.1007/BF00119960>, 1991.

330 Chapman, E. G., Gustafson, W. I., Easter, R. C., Barnard, J. C., Ghan, S. J., and Pekour, M. S.: Coupling aerosol-cloud-radiative processes  
331 in the WRF-Chem model: Investigating the radiative impact of elevated point sources, *Atmos. Chem. Phys.*, 9, 945–964,  
332 <https://doi.org/10.5194/acp-9-945-2009>, 2009.

333 Chen, Y. C., Christensen, M. W., Xue, L., Sorooshian, A., Stephens, G. L., Rasmussen, R. M., and Seinfeld, J. H.: Occurrence of lower  
334 cloud albedo in ship tracks, *Atmos. Chem. Phys.*, 12, 8223–8235, <https://doi.org/10.5194/acp-12-8223-2012>, 2012.

335 Di Vittorio, A. V. and Emery, W. J.: An automated, dynamic threshold cloud-masking algorithm for daytime AVHRR images over land,  
336 *IEEE Trans. Geosci. Remote Sensing*, 40, 1682–1694, <https://doi.org/10.1109/TGRS.2002.802455>, 2002.

337 Ding, A. J., Huang, X., Nie, W., Sun, J. N., Kerminen, V. - M., Petäjä, T., Su, H., Cheng, Y. F., Yang, X. - Q., Wang, M. H., Chi, X. G.,  
338 Wang, J. P., Virkkula, A., Guo, W. D., Yuan, J., Wang, S. Y., Zhang, R. J., Wu, Y. F., Song, Y., Zhu, T., Zilitinkevich, S., Kulmala, M.,  
339 and Fu, C. B.: Enhanced haze pollution by black carbon in megacities in China, *Geophys. Res. Lett.*, 43, 2873–2879,  
340 <https://doi.org/10.1002/2016gl067745>, 2016.

341 Ding, Q., Sun, J., Huang, X., Ding, A., Zou, J., Yang, X., and Fu, C.: Impacts of black carbon on the formation of advection–radiation fog  
342 during a haze pollution episode in eastern China, *Atmos. Chem. Phys.*, 19, 7759–7774, <https://doi.org/10.5194/acp-19-7759-2019>,  
343 2019.

344 Fan, J., Rosenfeld, D., Zhang, Y., Giangrande, S. E., Li, Z., and Machado, L. A. T.: Substantial convection and precipitation enhancements  
345 by ultrafine aerosol particles, *Science*, 359, 411–418, <https://doi.org/10.1126/science.aan8461>, 2018.

346 Fan, J., Wang, Y., Rosenfeld, D., and Liu, X.: Review of Aerosol–Cloud Interactions: Mechanisms, Significance, and Challenges, *J. Atmos.*  
347 *Sci.*, 73, 4221–4252, <https://doi.org/10.1175/JAS-D-16-0037.1>, 2016.

348 Fast, J. D., Gustafson, W. I., Easter, R. C., Zaveri, R. A., Barnard, J. C., Chapman, E. G., Grell, G. A., and Peckham, S. E.: Evolution of  
349 ozone, particulates, and aerosol direct radiative forcing in the vicinity of Houston using a fully coupled meteorology-  
350 chemistry-aerosol model, *J. Geophys. Res.*, 111, <https://doi.org/10.1029/2005jd006721>, 2006.

351 Goren, T. and Rosenfeld, D.: Satellite observations of ship emission induced transitions from broken to closed cell marine stratocumulus  
352 over large areas, *J. Geophys. Res.-Atmos.*, 117, -, <https://doi.org/10.1029/2012JD017981>, 2012.

353 Gu, Y., Kusaka, H., van Doan, Q., and Tan, J.: Impacts of urban expansion on fog types in Shanghai, China: Numerical experiments by  
354 WRF model, *Atmos. Res.*, 220, 57–74, <https://doi.org/10.1016/j.atmosres.2018.12.026>, 2019.

355 Gultepe, I., Tardif, R., Michaelides, S. C., Cermak, J., Bott, A., Bendix, J., Müller, M. D., Pagowski, M., Hansen, B., Ellrod, G., Jacobs, W.,  
356 Toth, G., and Cober, S. G.: Fog Research: A Review of Past Achievements and Future Perspectives, *Pure Appl. Geophys.*, 164, 1121–  
357 1159, <https://doi.org/10.1007/s00024-007-0211-x>, 2007.

358 Gultepe, I., Müller, M. D., and Boybeyi, Z.: A New Visibility Parameterization for Warm-Fog Applications in Numerical Weather Prediction  
359 Models, *J. Appl. Meteorol. Climatol.*, 45, 1469–1480, <https://doi.org/10.1175/jam2423.1>, 2006.

360 Gultepe, I., Milbrandt, J. A., and Zhou, B.: Marine fog: A review on microphysics and visibility prediction, in: Koraćin D., Dorman C. (eds)  
361 *Marine Fog: Challenges and Advancements in Observations, Modeling, and Forecasting*, Springer, Cham, 50 pp., 2017.

362 Guo, J., Su, T., Li, Z., Miao, Y., Li, J., Liu, H., Xu, H., Cribb, M., and Zhai, P.: Declining frequency of summertime local-scale precipitation  
363 over eastern China from 1970 to 2010 and its potential link to aerosols, *Geophys. Res. Lett.*, 44, 5700–5708,  
364 <https://doi.org/10.1002/2017GL073533>, 2017.

365 Guo, T., Zhu, B., Kang, Z., Gui, H., and Kang, H.: Spatial and temporal distribution characteristic of fog days and haze days from  
366 1960–2012 and impact factors over the Yangtze River Delta Region, *China Environmental Science*, 36, 961 – 969,  
367 <https://doi.org/10.3969/j.issn.1000-6923.2016.04.001>, 2016. [in Chinese]

368 IPCC: Climate change 2013: The physical science basis, Contribution of Working Group I to the Fifth Assessment Report of the Intergov-  
369 ernmental Panel on Climate Change, Cambridge University Press, Cambridge, United Kingdom and New York, NY, USA, 1585 pp.,  
370 2013.

371 Jia, X. and Guo X.: Impacts of Anthropogenic Atmospheric Pollutant on Formation and Development of a Winter Heavy Fog Event, Chi-  
372 nese Journal of Atmospheric Sciences, 36, 995–1008, <https://doi.org/10.3878/j.issn.1006-9895.2012.11200>, 2012. [in Chinese]

373 Jia, X. and Guo, X.: Impacts of Secondary Aerosols on a Persistent Fog Event in Northern China, Atmospheric and Oceanic Science Let-  
374 ters, 5, 401–407, <https://doi.org/10.1080/16742834.2012.11447022>, 2015.

375 Jia, X., Quan, J., Zheng, Z., Liu, X., Liu, Q., He, H., and Liu, Y.: Impacts of anthropogenic aerosols on fog in North China Plain, J. Ge-  
376 ophys. Res.-Atmos., 124, 252–265, <https://doi.org/10.1029/2018jd029437>, 2018.

377 Kang, H., Zhu, B., Zhu, T., Sun, J., and Ou, J.: Impact of Megacity Shanghai on the Urban Heat-Island Effects over the Downstream City  
378 Kunshan, Bound.-Layer Meteor., 152, 411–426, <https://doi.org/10.1007/s10546-014-9927-1>, 2014.

379 Khain, A. P. and Pinsky, M.: Modeling: A Powerful Tool for Cloud Investigation, in: Physical processes in clouds and cloud modeling,  
380 Cambridge University Press, Cambridge, United Kingdom and New York, NY, USA, 98 pp., 2018.

381 Koren, I., Martins, J. V., Remer, L. A., and Afargan, H.: Smoke invigoration versus inhibition of clouds over the Amazon, Science, 321,  
382 946–949, <https://doi.org/10.1126/science.1159185>, 2008.

383 Koschmieder, H.: Theorie der horizontalen sichtweite, Beitr Phys.d.freien Atm, 12, 171–181, 1924.

384 Kunkel, B. A.: Parameterization of Droplet Terminal Velocity and Extinction Coefficient in Fog Models, J. Appl. Meteorol., 23, 34–41,  
385 [https://doi.org/10.1175/1520-0450\(1984\)023<0034:PODTVA>2.0.CO;2](https://doi.org/10.1175/1520-0450(1984)023<0034:PODTVA>2.0.CO;2), 1983

386 LaDochy, S.: The Disappearance of Dense Fog in Los Angeles: Another Urban Impact?, Phys. Geogr., 26, 177–191,  
387 <https://doi.org/10.2747/0272-3646.26.3.177>, 2005.

388 Lee, T. F.: Urban clear islands in California central valley fog, Mon. Weather Rev., 115, 1794–1796,  
389 [https://doi.org/10.1175/1520-0493\(1987\)1152.0.CO;2](https://doi.org/10.1175/1520-0493(1987)1152.0.CO;2), 1987.

390 Leng, C., Zhang, Q., Zhang, D., Xu, C., Cheng, T., Zhang, R., Tao, J., Chen, J., Zha, S., and Zhang, Y.: Variations of cloud condensation  
391 nuclei (CCN) and aerosol activity during fog-haze episode: a case study from Shanghai, Atmos. Chem. Phys., 14, 12499–12512,  
392 <https://doi.org/10.5194/acp-14-12499-2014>, 2014.

393 Li, Y., Cao, L., Gao, S., and Luo, B.: The Current Stage and Development of MICAPS, Meteorological Monthly, 36, 50–55, 2010. [in Chi-  
394 nese]

395 Li, Z., Guo, J., Ding, A., Liao, H., Liu, J., Sun, Y., Wang, T., Xue, H., Zhang, H., and Zhu, B.: Aerosol and boundary-layer interactions and  
396 impact on air quality, Natl. Sci. Rev., 4, 810–833, <https://doi.org/10.1093/nsr/nwx117>, 2017.

397 Li, Z., Lau, W. K. M., Ramanathan, V., Wu, G., Ding, Y., Manoj, M. G., Liu, J., Qian, Y., Li, J., Zhou, T., Fan, J., Rosenfeld, D., Ming, Y.,  
398 Wang, Y., Huang, J., Wang, B., Xu, X., Lee, S. S., Cribb, M., Zhang, F., Yang, X., Zhao, C., Takemura, T., Wang, K., Xia, X., Yin, Y.,  
399 Zhang, H., Guo, J., Zhai, P. M., Sugimoto, N., Babu, S. S., and Brasseur, G. P.: Aerosol and monsoon climate interactions over Asia,  
400 Rev. Geophys., 54, 866–929, <https://doi.org/10.1002/2015RG000500>, 2016.

401 Li, Z., Yang, J., Shi, C., and Pu, M.: Urbanization Effects on Fog in China: Field Research and Modeling, Pure Appl. Geophys., 169, 927–  
402 939, <https://doi.org/10.1007/s00024-011-0356-5>, 2011.

403 Liu, H., Guo, J., Koren, I., Altaratz, O., Dagan, G., Wang, Y., Jiang, J. H., Zhai, P., and Yung, Y. L.: Non-Monotonic Aerosol Effect on  
404 precipitation in Convective Clouds over tropical oceans. Sci. Rep., 9, 1–7, <https://doi.org/10.1038/s41598-019-44284-2>, 2019.

405 Maalick, Z., Kühn, T., Korhonen, H., Kokkola, H., Laaksonen, A., and Romakkaniemi, S.: Effect of aerosol concentration and absorbing  
406 aerosol on the radiation fog life cycle, Atmos. Environ., 133, 26–33, <https://doi.org/10.1016/j.atmosenv.2016.03.018>, 2016.

407 Morrison, H., Curry, J. A., and Khvorostyanov, V. I.: A new double-moment microphysics parameterization for application in cloud and  
408 climate models. Part I: Description, J. Atmos. Sci., 62, 1665–1677, <https://doi.org/10.1175/JAS3446.1>, 2005.

409 Naira Chaouch, Marouane Temimi, Michael Weston, and Hosni Ghedira: Sensitivity of the meteorological model WRF-ARW to planetary  
410 boundary layer schemes during fog conditions in a coastal arid region, Atmos. Res., 187, 106–127,  
411 <https://doi.org/10.1016/j.atmosres.2016.12.009>, available at: <http://www.sciencedirect.com/science/article/pii/S0169809516307116>,  
412 2017.

413 Niu, F., Li, Z., Li, C., Lee, K., and Wang, M.: Increase of wintertime fog in China: Potential impacts of weakening of the Eastern Asian  
414 monsoon circulation and increasing aerosol loading, J. Geophys. Res., 115, <https://doi.org/10.1029/2009jd013484>, 2010a.

415 Niu, S., Lu, C., Yu, H., Zhao, L., and Lü, J.: Fog research in China: An overview, *Adv. Atmos. Sci.*, 27, 639–662,  
416 <https://doi.org/10.1007/s00376-009-8174-8>, 2010b.

417 Rangognio, J.: Influence of aerosols on the formation and development of radiation fog, *Atmos. Chem. Phys.*, 9, 17963–18019,  
418 <https://doi.org/10.5194/acpd-9-17963-2009>, 2009.

419 Rosenfeld, D., Meinrat O. Andreae, Asmi, A., Chin, M., and Johannes Quaas: Global observations of aerosol-cloud-precipitation-climate  
420 interactions, *Rev. Geophys.*, 52, 750–808, <https://doi.org/10.1002/2013RG000441>, 2014.

421 Rosenfeld, D., Lohmann, U., Raga, G. B., O’Dowd, C. D., Kulmala, M., Fuzzi, S., Reissell, A., and Andreae, M. O.: Flood or drought:  
422 how do aerosols affect precipitation?, *Science*, 321, 1309–1313, <https://doi.org/10.1126/science.1160606>, 2008.

423 Rozoff, C. M., Cotton, W. R., and Adegoke, J. O.: Simulation of St. Louis, Missouri, Land Use Impacts on Thunderstorms, *J. Appl. Meteorol.*, 42, 716–738, [https://doi.org/10.1175/1520-0450\(2003\)042<0716:SOSLML>2.0.CO;2](https://doi.org/10.1175/1520-0450(2003)042<0716:SOSLML>2.0.CO;2), 2003.

424 Sachweh, M. and Koepke, P.: Radiation fog and urban climate, *Geophys. Res. Lett.*, 22, 1073–1076, <https://doi.org/10.1029/95gl00907>,  
425 1995.

426 Shepherd, J. M.: A Review of Current Investigations of Urban-Induced Rainfall and Recommendations for the Future, *Earth Interact.*, 9,  
427 1–27, <https://doi.org/10.1175/ei156.1>, 2005.

428 Shi, C., Roth, M., Zhang, H., and Li, Z.: Impacts of urbanization on long-term fog variation in Anhui Province, China, *Atmos. Environ.*, 42,  
429 8484–8492, <https://doi.org/10.1016/j.atmosenv.2008.08.002>, 2008.

430 Stolaki, S., Haefelin, M., Lac, C., Dupont, J. C., Elias, T., and Masson, V.: Influence of aerosols on the life cycle of a radiation fog event.  
431 A numerical and observational study, *Atmos. Res.*, 151, 146–161, <https://doi.org/10.1016/j.atmosres.2014.04.013>, 2015.

432 Tao, W. K., Chen, J. P., Li, Z., Wang, C., and Zhang, C.: Impact of aerosols on convective clouds and precipitation, *Rev. Geophys.*, 50,  
433 6837, <https://doi.org/10.1029/2011RG000369>, 2012.

434 Tie, X., Huang, R., Cao, J., Zhang, Q., Cheng, Y., Su, H., Chang, D., Pöschl, U., Hoffmann, T., Dusek, U., Li, G., Worsnop, D., and  
435 O’Dowd, C.: Severe Pollution in China Amplified by Atmospheric Moisture, *Sci. Rep.* 7, 15760,  
436 <https://doi.org/10.1038/s41598-017-15909-1>, 2017.

437 Tie, X., Long, X., Li, G., Zhao, S., Cao, J., and Xu, J.: Ozone enhancement due to photo-dissociation of nitrous acid in eastern China, *Atmos. Chem. Phys.*, 19, 11267–11278, <https://doi.org/10.5194/acp-19-11267-2019>, 2019.

438 Twomey, S. A.: The Influence of Pollution on the Shortwave Albedo of Clouds, *J. Atmos. Sci.*, 34, 1149–1154,  
439 [https://doi.org/10.1175/1520-0469\(1977\)034<1149:tiopot>2.0.co;2](https://doi.org/10.1175/1520-0469(1977)034<1149:tiopot>2.0.co;2), 1977.

440 Wang, F., Guo, J., Zhang, J., Huang, J., Min, M., Chen, T., Liu, H., Deng, M., and Li, X.: Multi-sensor quantification of aerosol-induced  
441 variability in warm clouds over eastern China, *Atmos. Environ.*, 113, 1–9, <https://doi.org/10.1016/j.atmosenv.2015.04.063>, 2015

442 Yan, S., Zhu, B., and Kang, H.: Long-term fog variation and its impact factors over polluted regions of East China, *J. Geophys. Res.-Atmos.*, 124, 1741–1754, <https://doi.org/10.1029/2018JD029389>, 2019.

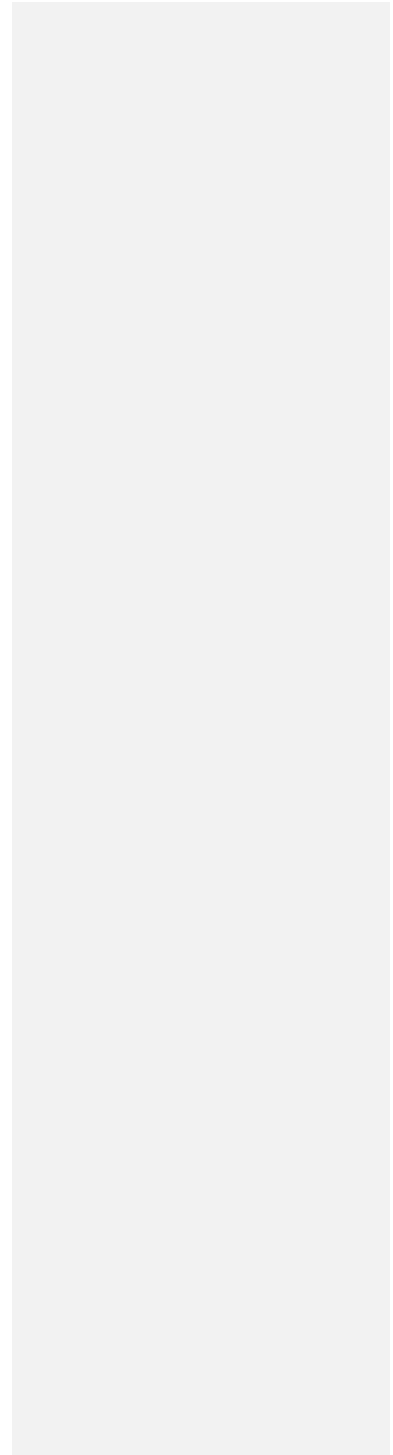
443 Yang, Y., Hu, X., Gao, S., and Wang, Y.: Sensitivity of WRF simulations with the YSU PBL scheme to the lowest model level height for a  
444 sea fog event over the Yellow Sea, *Atmos. Res.*, 215, 253–267, <https://doi.org/10.1016/j.atmosres.2018.09.004>, 2019.

445 Zhang, N. and Ma, X.: Analysis of the June 2018 Atmospheric Circulation and Weather, *Meteorological Monthly*, 43, 508– 512,  
446 <https://doi.org/10.7519/j.issn.1000-0526.2017.04.014>, 2017. [in Chinese]

447 Zhang, X., Musson-Genon, L., Dupont, E., Milliez, M., and Carissimo, B.: On the Influence of a Simple Microphysics Parametrization on  
448 Radiation Fog Modelling: A Case Study During ParisFog, *Bound.-Layer Meteor.*, 151, 293–315,  
449 <https://doi.org/10.1007/s10546-013-9894-y>, 2014.

450 Zhu, B. and Guo, T.: Review of the Impact of Air Pollution on Fog, *Advances in Meteorological Science and Technology*, 6, 56– 63,  
451 <https://doi.org/10.3969/j.issn.2095-1973.2016.02.006>, 2016. [in Chinese]

452 Zhu, J., Zhu, B., Huang, Y., An, J., and Xu, J.: PM2.5 vertical variation during a fog episode in a rural area of the Yangtze River Delta,  
453 China, *Sci. Total Environ.*, 685, 555–563, <https://doi.org/10.1016/j.scitotenv.2019.05.319>, 2019.



458 Table 1. Summary of major parameterization schemes.

Scheme	Option
Boundary layer	YSU
Longwave radiation	RRTM
Shortwave radiation	New Goddard
Microphysics	Morrison
Surface layer	MM5 similarity
Land surface	Noah
Urban surface	Urban canopy model
Gas phase chemistry	CBMZ
Aerosol chemistry	MOSAIC (4-bin)
Aerosol-cloud and aerosol-radiation interactions	All turned on
Aerosol activation	Abdul-Razzak and Ghan (2002)

批注 [yansq18]: Reference#1\_Comment1

459

460

461 Table 2. Settings of sensitive experiments. "N" represents no changes.

Case name	Description	Underlying surface	Anthropogenic emission
u0e0	base condition	N	N
u3e0	urbanization condition	the 11x13 grid centered on SX is replaced by urban surface	N
u0e3	polluted condition	N	the 11x13 grid centered on SX is replaced by the emission of Hefei downtown
u3e3	urbanization and polluted condition	same as u3e0	same as u0e3

Effect	Description
u3e0-u0e0	urbanization effect
u0e3-u0e0	aerosol effect
u3e3-u0e0	urbanization and aerosol effect

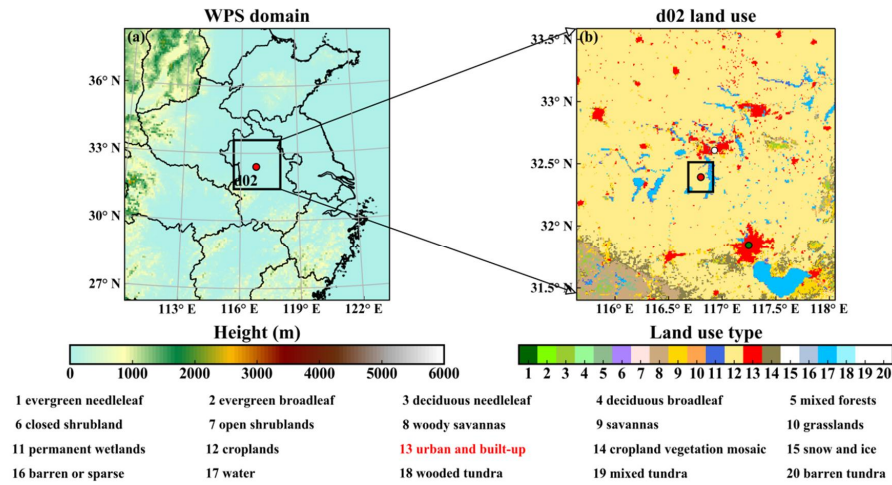
462

463

464

465

466

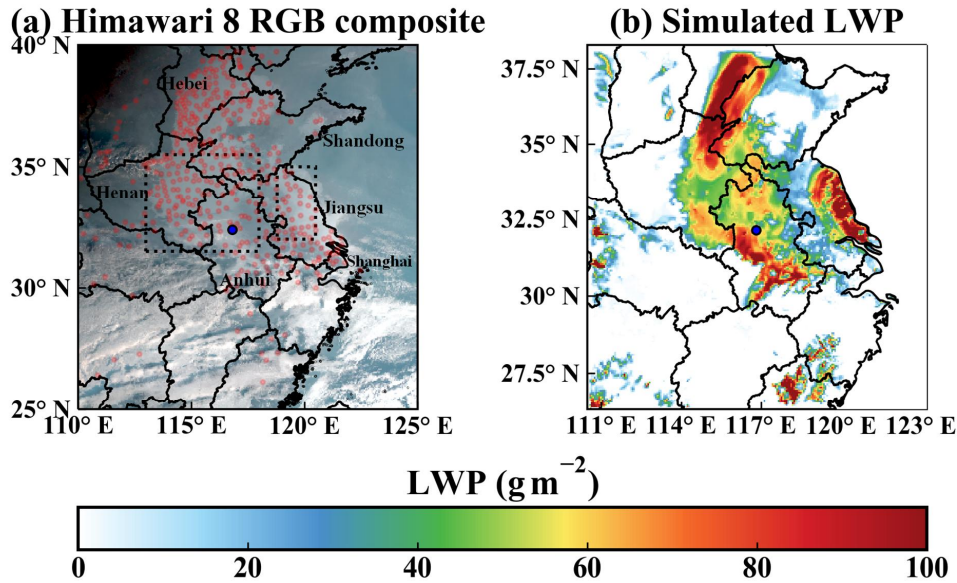


468

469 Figure 1. (a) The WRF domain overlaid with terrain height. (b) The land use distribution of domain d02. The green dot  
 470 is Hefei, the capital of Anhui Province. The white dot is Huainan. The two red dots are the SX site. The land use and  
 471 emissions of the 22 km × 26 km black box in the center of (b) will be altered in the sensitivity experiments.

472

批注 [yansq19]: Refer-  
 eef#1\_Comment8



474

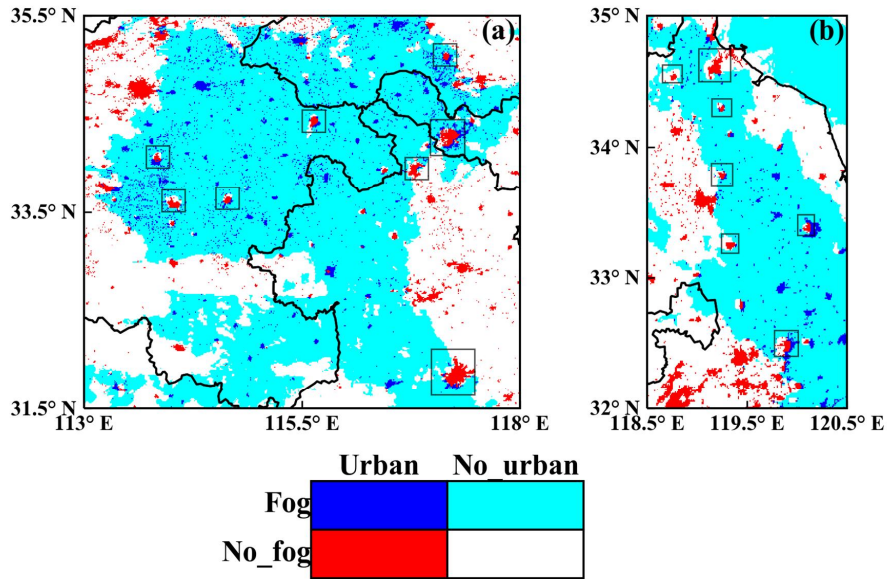
475 | Figure 2. The performance of the simulated fog zone at 08:00 03 January 2017. (a) Himawari 8 RGB composite cloud  
 476 | image overlaid with the MICAPS observation sites (light red dots) at which fog was observed (relative humidity > 90 %  
 477 | and VIS < 1 km). (b) Simulated LWP distribution. Only LWC below 1500 m are integrated. The blue dots are the SX  
 478 | site. The two dashed rectangles in (a) are the subregions of interest in Fig. 3.

479

批注 [yansq20]: Refer-  
 eef#1\_Comment15

批注 [yansq21]: Refer-  
 eef#1\_Comment16

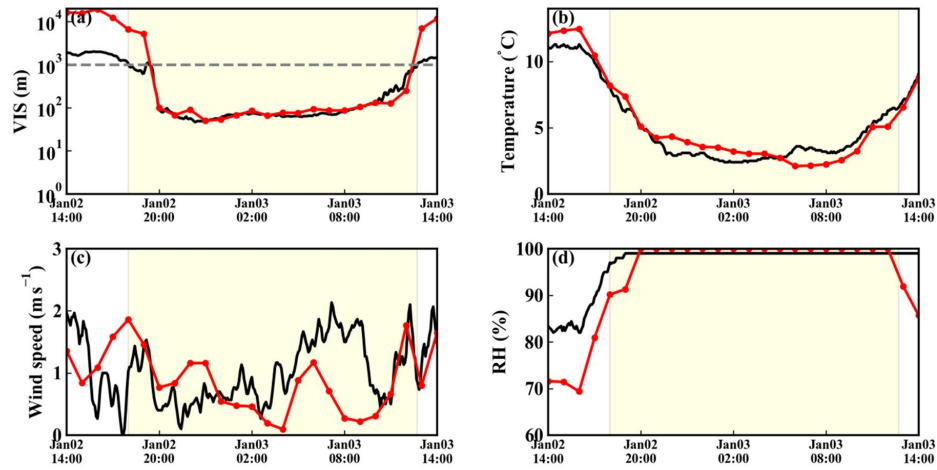




481

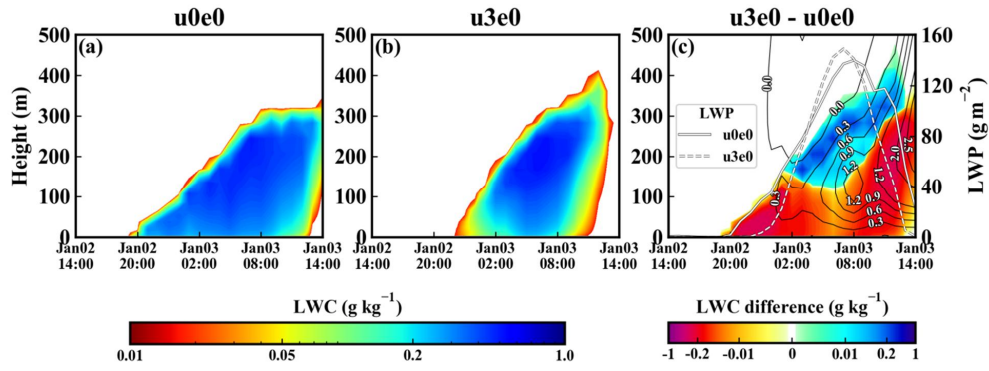
482 | Figure 3. Two sub-regions (a and b) with obvious fog holes on the Himawari 8 image at 11:00 03 January 2017. The  
 483 | fog zone, which is represented by albedo  $> 0.45$  (at  $0.64 \mu\text{m}$ ) and brightness temperature  $> 266 \text{ K}$  (at  $12.4 \mu\text{m}$ ) (Di  
 484 | Vittorio et al., 2002), is marked with cold colours (blue or cyan). The urban areas are marked with blue or red. The red  
 485 | and white pixels surrounded or semi-surrounded by cold colours are fog holes, and among these pixels, the red pixels  
 486 | indicate the fog holes over urban areas. Some of the cities with fog holes are marked by rectangles.  
 487

批注 [yansq22]: Refer-  
 eef#1\_Comment16



489

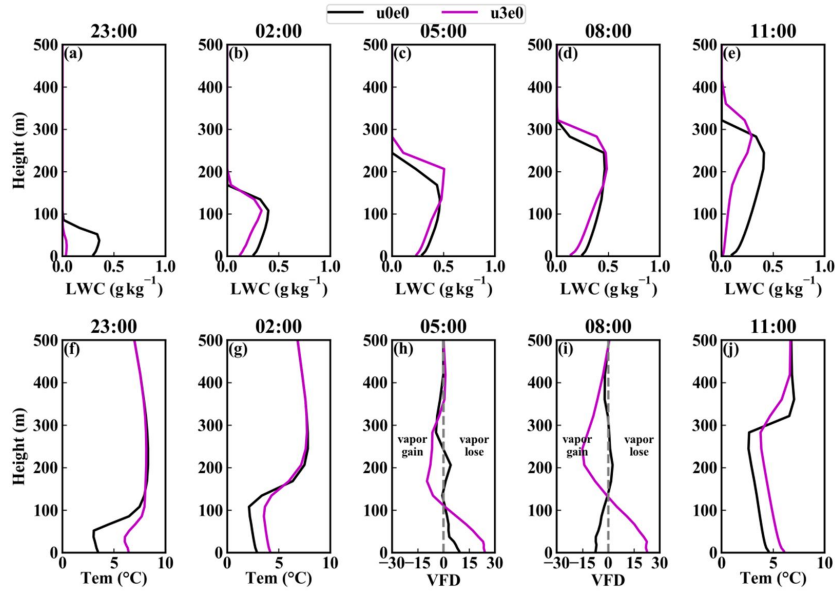
490 Figure 4. The performance of the simulated meteorological parameters at the SX site. (a) VIS. (b) air temperature. (c)  
 491 10-minute average wind speed. (d) Relative humidity (RH). The red dotted lines represent the model results, and the  
 492 black lines are the observations. The fog period (VIS < 1 km and RH > 90 %) is shaded with light yellow.  
 493



495

496 Figure 5. Time-height distribution of the LWC ( $\text{g kg}^{-1}$ ) in (a) u0e0 and (b) u3e0, and (c) is the urbanization effect (u3e0  
 497 minus u0e0) on LWC. The two white curves in (c) are the LWP. The black contour lines in (c) are the difference of  
 498 vertical velocity ( $\text{cm s}^{-1}$ ) (u3e0 minus u0e0). Only the lines after 00:00 are shown for clarity.  
 499

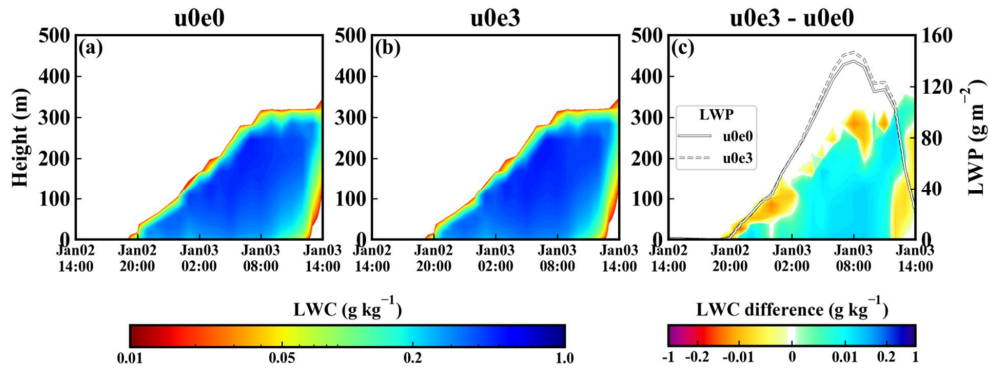
500



501

502 Figure 6. Profiles of the LWC (first row), temperature (Tem) (f, g, j) and vertical vapour flux divergence (VFD) (h, i)  
503 ( $\text{g h}^{-1} \text{m}^{-2} \cdot \text{hpa}^{-1}$ ) in u0e0 and u3e0 at different times.  
504

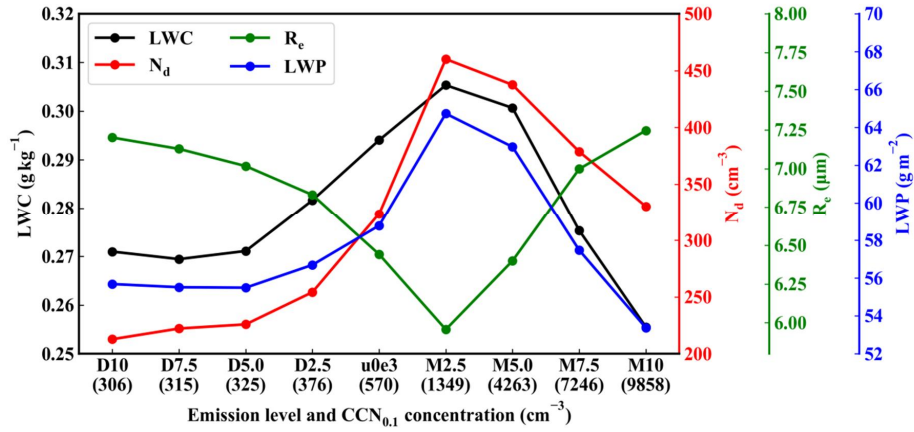
505



506

507 Figure 7. Similar to Fig. 5, but for the aerosol effect (u0e3 minus u0e0).

508



510

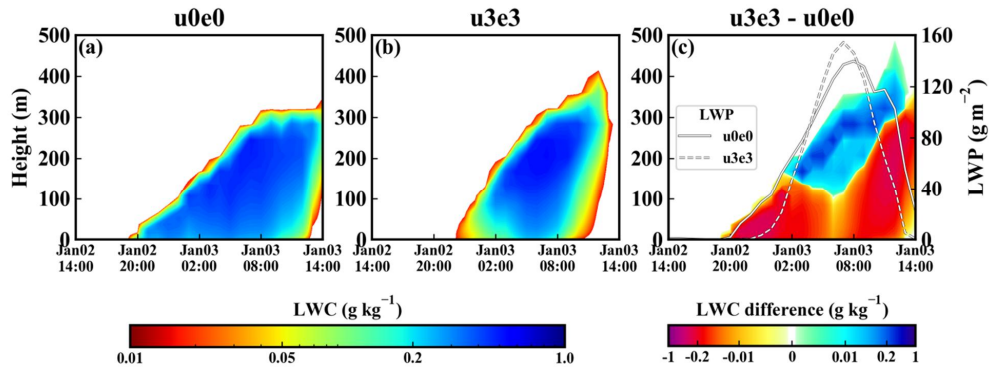
511 Figure 8. Relationships of the microphysical parameters (LWC, N<sub>d</sub>, R<sub>e</sub> and LWP) with emission level and CCN<sub>0.1</sub> con-  
 512 centrations. These parameters are the time-height averages (time average for the LWP) in fog, taking only non-zero  
 513 values into consideration.

514

批注 [yansq23]: CCN<sub>0.1</sub> is marked under the corresponding experiments

批注 [yansq24]: Refer-  
 ee#1\_Comment12 & 13

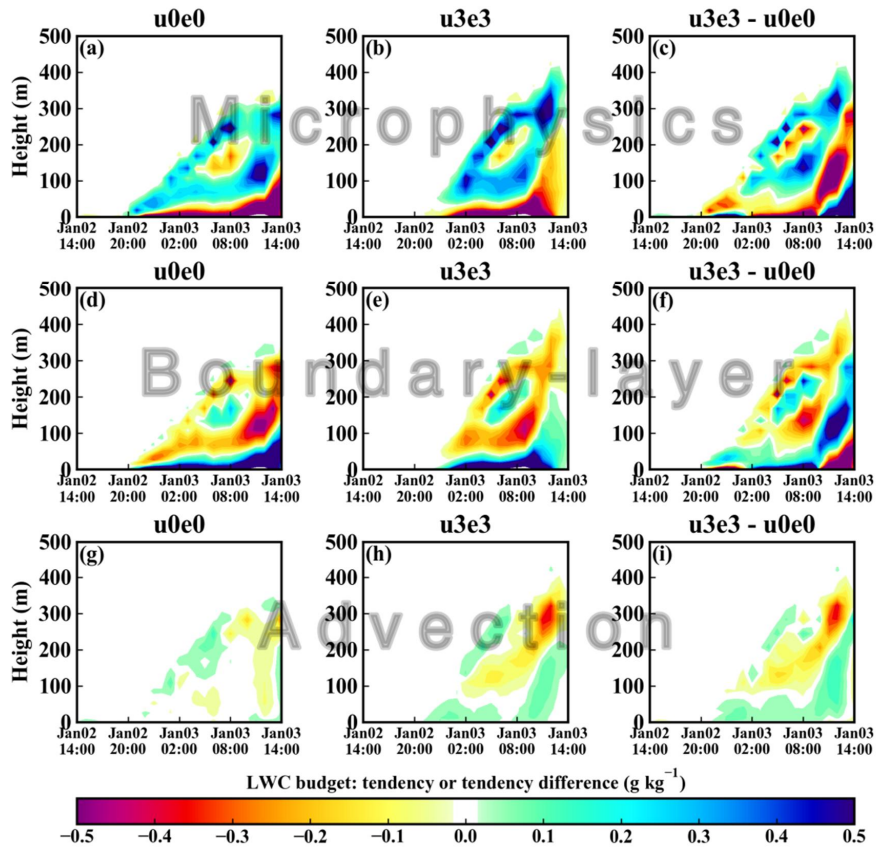
515



516

517 Figure 9. Similar to Fig. 5, but for the combined effect of urbanization and aerosols ( $u3e3$  minus  $u0e0$ ).

518



520

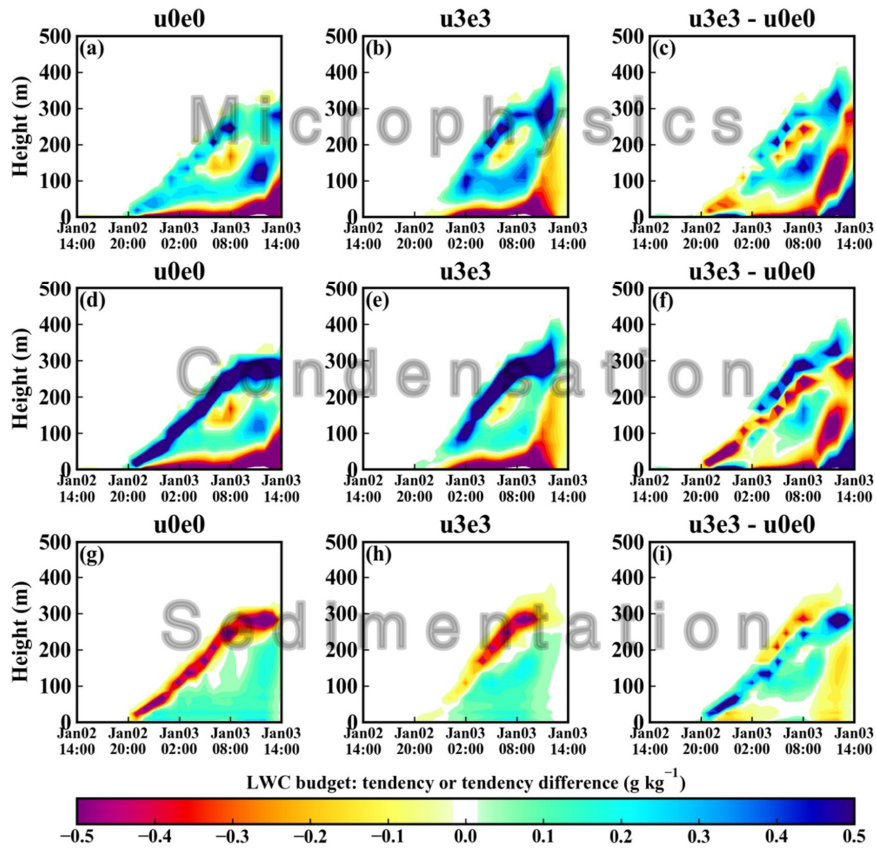
521 Figure 10. The combined effect of urbanization and aerosols (u3e3 minus u0e0) on various items of the LWC budget.

522 | The three rows are the ~~1-hour-accumulated~~hourly tendencies ( $\text{g kg}^{-1}$ ) of the microphysical, boundary layer, and advec-

523 tion processes.

524





526

527 Figure 11. The combined effect of urbanization and aerosols (u3e3 minus u0e0) on various items of the microphysical  
 528 tendency. The three rows are the ~~1-hour accumulated~~hourly tendencies ( $\text{g kg}^{-1}$ ) of the microphysical,  
 529 condensation/evaporation, and sedimentation processes.

530